DD and HD Models for Noise due to Impact Ionization in Si and SiGe Devices Verified by MC Simulations

B. Neinhüs, C. Jungemann, and B. Meinerzhagen

Institut für Theoretische Elektrotechnik und Mikroelektronik
Universität Bremen, Kufsteiner Straße, Postfach 33 04 40, 28334 Bremen, Germany
Tel.: +49 421 218 4689, Fax: +49 421 218 4434, E-Mail: neinhus@item.uni-bremen.de

ABSTRACT

An efficient model for the simulation of terminal current noise in the presence of avalanche carrier generation is presented. Our approach is investigated by DD, HD, and MC noise simulations of a 1D N^+NN^+ structure. A comparison of the terminal current noise evaluated by the 2D HD and DD Langevin equations with full band Monte Carlo simulations exhibits excellent agreement between the MC and HD results.

Keywords: noise, device simulation, impact ionization

INTRODUCTION

The rapid proliferation of Si and SiGe devices for radio-frequency (RF) applications [1] has caused a demand for physics-based noise modeling and recently the first hierarchical 2D bipolar drift-diffusion (DD) and hydrodynamic (HD) noise models for multi-terminal Si and SiGe devices have been developed [2, 3]. The inclusion of noise due to the generation of secondary particles by impact ionization (II) into these models and the verification by full-band Monte Carlo (MC) simulations are demonstrated in this paper for the first time.

MODELS

In order to simulate noise with our DD and HD models, the DD and HD Langevin equations must be solved. These are derived along the same lines as the DD and HD models [4] where each balance equation includes an additional Langevin force. The respective equations of the DD and HD model must be solved self-consistently with Poisson's equation.

HD model

$$\nabla_{\vec{r}}^{\mathrm{T}}\vec{j}_p = -\frac{\partial p}{\partial t} + G^{II} + \xi_{\dot{p}} \tag{1}$$

$$\vec{j}_p = \mu_{\mathrm{p}}^*\left[p\nabla_{\vec{r}}\tilde{\Psi} - q\frac{\tau_{\vec{j}_{\mathrm{p}}}}{\tau_{\vec{j}_{\mathrm{p}}}^*}\Big(\nabla_{\vec{r}}(p\,U_{T_{\mathrm{p}}^*}) - p\,U_{T_{\mathrm{p}}^*}\frac{\nabla_{\vec{r}}N_{\mathrm{v}}}{N_{\mathrm{v}}}\Big)\right] + \vec{\xi}_{\vec{j}_p} \tag{2}$$

$$\nabla_{\vec{r}}^{\mathrm{T}}\vec{s}_p = q\vec{j}_p\nabla_{\vec{r}}\tilde{\Psi} - p\,\frac{3}{2}k_B\frac{T_p^* - T_0}{\tau_{w_{\mathrm{p}}}^*} + \xi_{\dot{w}_p} \tag{3}$$

$$\vec{s}_p = q\mu_{s_{\mathrm{p}}}^*\left[\nabla_{\vec{r}}\tilde{\Psi} - \frac{\tau_{\vec{j}_{\mathrm{p}}}}{\tau_{\vec{j}_{\mathrm{p}}}^*}\Big(2p\nabla_{\vec{r}}U_{T_{\mathrm{p}}^*} + U_{T_{\mathrm{p}}^*}\nabla_{\vec{r}}p - p\,U_{T_{\mathrm{p}}^*}\frac{\nabla_{\vec{r}}N_{\mathrm{v}}}{N_{\mathrm{v}}}\Big)\right] + \vec{\xi}_{\vec{s}_p} \tag{4}$$

$$\nabla_{\vec{r}}^{\mathrm{T}}\vec{j}_n = -\frac{\partial n}{\partial t} + G^{II} + \xi_{\dot{n}} \tag{5}$$

$$\vec{j}_n = \mu_{\mathrm{n}}^*\left[-n\nabla_{\vec{r}}\tilde{\Psi} - q\frac{\tau_{\vec{j}_{\mathrm{n}}}}{\tau_{\vec{j}_{\mathrm{n}}}^*}\Big(\nabla_{\vec{r}}(n\,U_{T_{\mathrm{n}}^*}) - n\,U_{T_{\mathrm{n}}^*}\frac{\nabla_{\vec{r}}N_{\mathrm{c}}}{N_{\mathrm{c}}}\Big)\right] + \vec{\xi}_{\vec{j}_n} \tag{6}$$

$$\nabla_{\vec{r}}^{\mathrm{T}}\vec{s}_n = -q\vec{j}_n\nabla_{\vec{r}}\tilde{\Psi} - n\,\frac{3}{2}k_B\frac{T_n^* - T_0}{\tau_{w_{\mathrm{n}}}^*} + \xi_{\dot{w}_n} \tag{7}$$

$$\vec{s}_n = q\mu_{s_{\mathrm{n}}}^*\left[-\nabla_{\vec{r}}\tilde{\Psi} - \frac{\tau_{\vec{j}_{\mathrm{p}}}}{\tau_{\vec{j}_{\mathrm{n}}}^*}\Big(2p\nabla_{\vec{r}}U_{T_{\mathrm{n}}^*} + U_{T_{\mathrm{n}}^*}\nabla_{\vec{r}}n - n\,U_{T_{\mathrm{n}}^*}\frac{\nabla_{\vec{r}}N_{\mathrm{c}}}{N_{\mathrm{c}}}\Big)\right] + \vec{\xi}_{\vec{s}_n} \tag{8}$$

DD model

$$\nabla_{\vec{r}}^{\mathrm{T}}\vec{j}_p = -\frac{\partial p}{\partial t} + G^{II} + \xi_{\dot{p}} \tag{9}$$

$$\vec{j}_p = q\mu_{\mathrm{n}}^*\left[p\nabla_{\vec{r}}\tilde{\Psi} - U_{T_0}\nabla_{\vec{r}}p - U_{T_0}\frac{\nabla_{\vec{r}}N_{\mathrm{v}}}{N_{\mathrm{v}}}\right] + \vec{\xi}_{\vec{j}_p} \tag{10}$$

$$\nabla_{\vec{r}}^{\mathrm{T}} \vec{j}_n = -\frac{\partial n}{\partial t} + G^{II} + \xi_{\dot{n}} \tag{11}$$

$$\vec{j}_n = q\mu_{\mathrm{n}}^* \left[-n\nabla_{\vec{r}}\tilde{\Psi} - U_{T_0}\nabla_{\vec{r}} n - U_{T_0}\frac{\nabla_{\vec{r}} N_{\mathrm{c}}}{N_{\mathrm{c}}} \right] + \vec{\xi}_{\vec{j}_n} \tag{12}$$

Poisson's equation

$$\nabla_{\vec{r}}(\epsilon\nabla_{\vec{r}}\Psi) = -q(N_D - N_A + p - n) \tag{13}$$

where q is the electron charge, k_B the Boltzmann constant, p, n the carrier densities, G^{II} the II generation rate and $N_{c/v}$ the effective density of states in the conduction/valence band. The potential $\tilde{\Psi}$ is defined as $\tilde{\Psi} = \frac{E_{c,v}}{q} - \Psi$ where $E_{c,v}$ is the conduction/valence band edge and Ψ the electrostatic potential. $\vec{j}$ and $\vec{s}$ denote the current and energy current density with the relaxation times $\tau^*_{w_{\mathrm{n,p}}}$, $\tau_{\vec{j}}$, and $\tau^*_{\vec{j}}$ and the (energy) mobilities μ^* and μ^*_s. The quantities $\xi_{\dot{n},\dot{p}}$, $\vec{\xi}_{\vec{j}}$, $\xi_{\dot{w}}$ and $\vec{\xi}_{\vec{s}}$ are the Langevin forces for the particle, current, energy, and energy current density. It should be noted that first order derivatives in time have been neglected in all balance equations besides (1), (5), (9), and (11), which limits the validity of this approach to frequencies below 100 GHz.

The DD and HD noise equations are solved in the frequency domain by using a generalized Green's function approach [3,5,6]. The discretized Green's functions are computed by a method first suggested by Branin [7] which significantly enhances the computational efficiency of the algorithm. The described method has already been applied to consistently compute HD and DD diffusion noise [3, 8]. Our new approach to include II noise in the DD and HD models is a generalization of the method for generation noise outlined in [9] for the DD model. Since II generates secondary electrons and holes, the Langevin forces for $\xi_{\dot{p}}$ and $\xi_{\dot{n}}$ must be considered, whereas the contribution of II to the other Langevin forces $\vec{\xi}_{\vec{j}}$, $\xi_{\dot{w}}$ and $\vec{\xi}_{\vec{s}}$ can be neglected because the II scattering rate is small compared to the rates of the other scattering processes [10]. For II, secondary electrons and holes are always generated as pairs and are therefore correlated. As the generation of electron/hole pairs by II is a Poisson process the corresponding terminal current noise can be evaluated as

$$\underline{S}^{II}_{I_l I_k} = \int (\underline{G}^{\dot{p}}_{\delta I_l} + \underline{G}^{\dot{n}}_{\delta I_l}) 2G^{II} (\underline{G}^{\dot{p}}_{\delta I_k} + \underline{G}^{\dot{n}}_{\delta I_k})^* d^3r \tag{14}$$

where $\underline{G}^{\dot{p}}_{\delta I_l}$ and $\underline{G}^{\dot{n}}_{\delta I_l}$ are the Fourier transformed terminal current Green's functions corresponding to the Langevin forces $\xi_{\dot{p}}$ and $\xi_{\dot{n}}$ mentioned above. $\underline{G}^{\dot{p}}_{\delta I_l}(\vec{r},\omega)$ and $\underline{G}^{\dot{n}}_{\delta I_l}(\vec{r},\omega)$ are given by the current at the lth terminal due to a unit electron (hole) current injected with frequency ω at the position $\vec{r}$ within the device.

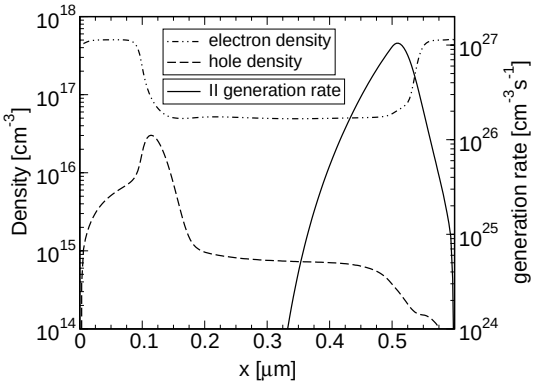

Figure 1: Electron density and II generation rate biased at 6V at room temperature evaluated by MC simulation

Noise due to particle scattering within the conduction or valence bands (diffusion noise) is included as described in [3].

RESULTS

In Fig. 1 the electron density, the II generation rate, and the density of the secondary holes are shown for a 1D Si N^+NN^+ structure (100nm doped with $5 \cdot 10^{17}/\mathrm{cm}^3$ followed by 400nm with $2 \cdot 10^{15}/\mathrm{cm}^3$ and again 100nm with $5 \cdot 10^{17}/\mathrm{cm}^3$) biased at 6V as calculated by the self-consistent MC model. About 1000 uniformly weighted test particles were simulated for 0.5μs.

The absolute value of the corresponding autocorrelation function (ACF) of the terminal current is shown in Fig. 2 as calculated with and without II. Below 1ps the ACFs show the usual oscillatory behavior due to plasma oscillations. In case II is considered, a distinct exponential tail with a time constant of about 27ps is observed beyond 10ps, which can not be found without II. This very long tail of about 100ps necessitated the extremely long MC simulation time of 0.5μs requiring about 19

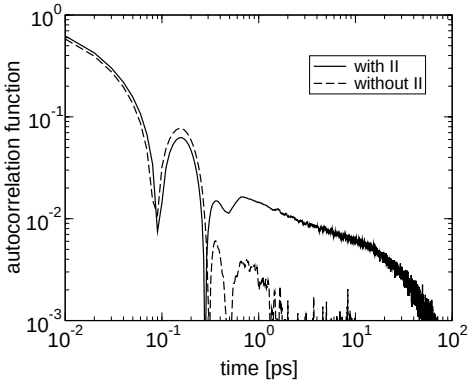

Figure 2: Absolute value of the ACF of the terminal current biased at 6V at room temperature evaluated by MC simulations with and without II, where the sign of the ACF is indicated

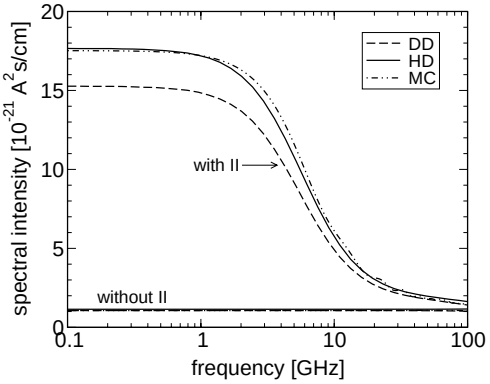

Figure 3: Spectral intensity of the terminal current biased at 6V at room temperature evaluated by MC, HD, DD simulations with and without II

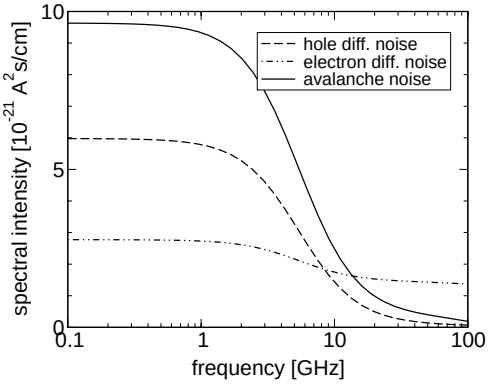

Figure 4: Contribution of avalanche, hole, and electron noise to the spectral intensity of the terminal current biased at 6V at room temperature evaluated by HD simulations

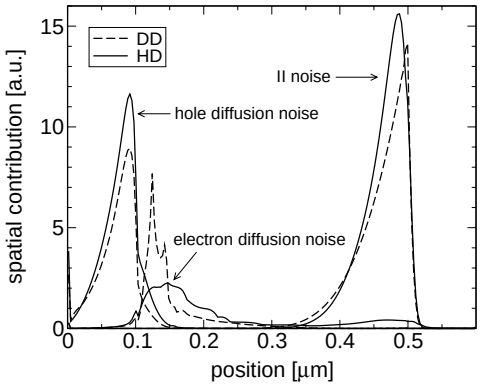

Figure 5: Spatial contribution of the different local noise sources to the low-frequency terminal current noise biased at 6V at room temperature evaluated by HD and DD simulations

CPU days on a 1GHz PC. This makes MC simulation of this effect in 2D devices very challenging, because 2D simulations are in general more CPU-intensive than 1D simulations.

The time tail of the ACF predominantly influences the low frequency part of the corresponding spectral intensity of the terminal current which is the Fourier transform of the ACF. This leads to the large deviations for S_{II} with and without II at low frequencies which can be observed in Fig. 3. The results are shown for the DD, HD and MC models where the frequency has been limited to the technically important range below 100GHz. For a meaningful comparison, the parameters of the DD and HD II models have been adjusted in such a way that the device-integrated II generation rate of the MC model is reproduced. Overall, excellent agreement of the HD and MC models is found for the whole range of frequencies. Since the HD and DD models are solved in the frequency domain, the problem with the tail of the ACF does not occur and the required CPU times are only 30 (HD) and 15 (DD) seconds for the data shown in Fig. 3.

The contributions of the electron and hole diffusion noise together with the avalanche generation noise to the terminal current noise are shown in more detail in Fig. 4. The domination of avalanche noise for the lower frequencies is again clearly visible whereas the contribution of the hole and electron diffusion noise is mainly caused by the II-generated carriers.

The spatial contributions of the different local noise sources to the terminal current noise are shown in Fig. 5. This information can not be extraced from MC simulations and is shown here for the classical DD and HD models. The origin of the terminal current noise caused by the generation of the secondary particles is located at the peak of the II generation rate (cf. Fig. 1). The diffusion noise of the secondary holes (p-diff) peaks at the same position as the hole density, whereas the peak of the electron diffusion noise (n-diff) is on the left side of the low density region, where the electron gas still has a moderate temperature.

CONCLUSIONS

We have presented the first hierarchical investigation of noise due to II in Si devices and excellent agreement of our new HD model with the MC model is demonstrated, where the HD model is nearly five orders of magnitude faster than the MC model. The good agreement between MC and HD simulations indicate that the HD Langevin model might serve as reference model for the DD noise model.

Acknowledgment: The authors gratefully acknowledge the initial funding of this project by the semiconductor products sector of Motorola Inc.

REFERENCES

[1] A. Schüppen, "SiGe–HBTs for mobile communication", *Solid–State Electron.*, vol. 43, pp. 1373–1381,

1999.

[2] S. Decker, C. Jungemann, B. Neinhüs, and B. Meinerzhagen, "2d hierarchical radio-frequency noise modelling based on a Langevin-type drift-diffusion model and full-band Monte-Carlo generated local noise sources", in *Proc. SISPAD*, 2001, pp. 136–139.

[3] C. Jungemann, B. Neinhüs, S. Decker, and B. Meinerzhagen, "Hierarchical 2D RF noise simulation of Si and SiGe devices by Langevin-type DD and HD models based on MC generated noise parameters", in *IEDM Tech. Dig.*, Washington (USA), 2001, pp. 481–484.

[4] R. Thoma, A. Emunds, B. Meinerzhagen, H. J. Peifer, and W. L. Engl, "Hydrodynamic equations for semiconductors with nonparabolic bandstructures", *IEEE Trans. Electron Devices*, vol. 38, pp. 1343–1352, 1991.

[5] F. Bonani, G. Ghione, M. R. Pinto, and R. K. Smith, "An efficient approach to noise analysis through multidimentional physics-based models", *IEEE Trans. Electron Devices*, vol. 45, pp. 261–269, 1998.

[6] F. Bonani and G. Ghione, "Noise modeling for PDE based device simulations", in *Proc. ICNF*, Gainesville, FL, 2001, vol. 16, pp. 631–636.

[7] F. H. Branin, "Network sensitivity and noise analysis simplified", *IEEE Transactions on circuit theory*, vol. 20, pp. 285–288, 1973.

[8] S. Decker, C. Jungemann, B. Neinhüs, and B. Meinerzhagen, "An accurate and efficient methodology for rf noise simulations of nm-scale MOSFETs based on a Langevin–type drift–diffusion model", in *International Conference on Noise in Physical Systems and 1/f Fluctuations*, Gainesville (USA), 2001.

[9] F. Bonani and G. Ghione, "Generation–recombination noise modelling in semiconductor devices through population or approximate equivalent current density fluctuations", *Solid–State Electron.*, vol. 43, pp. 285–295, 1999.

[10] M. V. Fischetti, N. Sano, S. E. Laux, and K. Natori, "Full-band-structure theory of high-field transport and impact ionization of electrons and holes in Ge, Si, and GaAs", *IEEE J. Tech. Comp. Aided Design*, , no. 3, 1997.